

Dear Author,

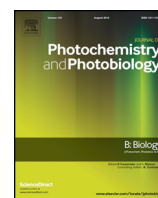
Please, note that changes made to the HTML content will be added to the article before publication, but are not reflected in this PDF.

Note also that this file should not be used for submitting corrections.



Contents lists available at ScienceDirect

Journal of Photochemistry & Photobiology, B: Biology

journal homepage: www.elsevier.com/locate/jpb1 Cryo-imaging of photosystems and phycobilisomes in *Anabaena sp. PCC 7120* cellsQ1 Gábor Steinbach^a, Félix Schubert^b, Radek Kaňa^{a,c,*}3 ^a Institute of Microbiology, CAS, Centrum Algatech, Třeboň, Czech Republic4 ^b Department of Mineralogy, Geochemistry and Petrology, Faculty of Science and Informatics, University of Szeged, Szeged, Hungary5 ^c Faculty of Science, Institute of Chemistry and Biochemistry, University of South Bohemia, Branišovská 31, 370 05 Ceske Budejovice, Czech Republic

7 A R T I C L E I N F O

8 Article history:

9 Received 29 May 2015

10 Received in revised form 2 October 2015

11 Accepted 5 October 2015

12 Available online xxxx

13 Keywords:

14 Confocal microscopy

15 Cryogenic microscopy

16 Cyanobacteria

17 Membrane domains

18 Photosynthesis

A B S T R A C T

Primary photosynthetic reactions take place inside thylakoid membrane where light-to-chemical energy conversion is catalyzed by two pigment-protein complexes, photosystem I (PSI) and photosystem II (PSII). Light absorption in cyanobacteria is increased by pigment-protein supercomplexes – phycobilisomes (PBSs) situated on thylakoid membrane surfaces that transfer excitation energy into both photosystems. We have explored the localization of PSI, PSII and PBSs in thylakoid membrane of native cyanobacteria cell *Anabaena sp. 7120* by means of cryogenic confocal microscopy. We have adapted a conventional temperature controlling stage to an Olympus FV1000 confocal microscope. The presence of red shifted emission of chlorophylls from PSI has been confirmed by spectral measurements. Confocal fluorescence images of PSI (in a spectral range 710–750 nm), PSII (in a spectral range 690–705 nm) and PBSs (in a spectral range 650–680 nm) were recorded at low temperature. Co-localization of images showed spatial heterogeneity of PSI, PSII and PBSs over the thylakoid membrane, and three dominant areas were identified: PSI-PSII-PBS supercomplex area, PSII-PBS supercomplex area and PSI area. The observed results were discussed with regard to light-harvesting regulation in cyanobacteria.

© 2015 Published by Elsevier B.V.

1. Introduction

Light-photosynthetic reactions in oxygenic phototrophs are catalyzed by two pigmented protein supercomplexes, photosystem I (PSI) and photosystem II (PSII). The photosystems work in succession during linear electron flow or separately in case of the cyclic electron flow around PSI. In higher plants, the text-book view proposes that PSII and PSI are separately distributed between granal and stromal thylakoids respectively [1]. However, it has been recently shown that a high portion of photosystems can also form a PSI-PSII megacomplex [2]. Thylakoid membrane heterogeneity in algal [3] or cyanobacterial cells is still rather questionable and a matter of intensive research [4–6]. The grana thylakoids in plants represent a fixed but flexible structure [7,8] where thylakoids are stacked by electrostatic interaction between photosynthetic complexes [9,10]. The physiological importance of thylakoid membrane heterogeneity is still not clear (see e.g. review [10]). One of the proposed ideas is that grana/stroma heterogeneity separates PSI from PSII that minimizes energy spillover from slower PSII into faster PSI [11]. Such a spatial separation of PSI and PSII in native thylakoid membranes of cyanobacteria has not been clearly shown [12–15], as the typical multilayer granal thylakoids are missing in

cyanobacteria (see e.g. [4,16]). The mechanism of how photosystems are co-localized (or separated) is still not satisfactorily described in cyanobacteria. Several models of PSI/PSII organization in cyanobacteria thylakoids have been already proposed (compare [5,6,13]). For instance, it has been suggested that PSI could be preferentially located either in the outermost thylakoids close to the cytoplasmic membrane *Synechococcus sp. 7942* [13] or in the inner membrane thylakoids of *Synechocystis sp. 6803* [6]. Electron microscopy methods have already indicated an existence of PSI/PSII separated domains where PSI and PSII are separated only by a few nanometers – PSII form arrays with PSIs on their periphery [12]. Recently, biochemical experiments with cross-linkers have indicated that both photosystems can in fact form a supercomplex with a single phycobilisome [17] that would indicate a rather minimal separation of photosystems. However, localization and abundance of such complexes is not known on a single cell level.

Life-cell imaging of small, micrometer-size cyanobacteria is a challenging task [18]. Localization of PSII and phycobilisomes in native cyanobacteria cells can be done straightforward as both proteins represent highly autofluorescent protein complexes. In contrast, PSI is in fact rather weakly fluorescent at room temperature [19]. Therefore, to access a spatial distribution of the photosystems and phycobilisomes, special experimental methods are required. Several methods have been already tested, including anti-Stokes Fluorescence spectroscopy [20, 21], combination of electron microscopy and immunochemistry [13], hyperspectral confocal fluorescence microscopy [4–6] and recently also cryogenic confocal microscopy (see e.g. [22]). These methods are based on different principles and require different instrumentations.

Abbreviations: PBS, phycobilisome; PSI, photosystem I; PSII, photosystem II.

* Corresponding author at: Institute of Microbiology, CAS, Centrum Algatech, Třeboň, Czech Republic.

E-mail addresses: steinbach@alga.cz (G. Steinbach), schubert@geo.u-szeged.hu (F. Schubert), kana@alga.cz (R. Kaňa).<http://dx.doi.org/10.1016/j.jphotobiol.2015.10.003>

1011-1344/© 2015 Published by Elsevier B.V.

For Anti-Stokes Fluorescence spectroscopy a continuous-wave IR laser at 800–820 nm is needed. With this it is possible to visualize lowest-energy traps that are typical for PSI [20,23]. Hyperspectral confocal fluorescence microscopy [6,24] provides another interesting opportunity to access the localization of photosystems and phycobilisomes simultaneously in single cells [4–6]; however it requires a minimal spectral overlap for spectra deconvolution that cannot be fulfilled for all organisms. However, in all these experimental methods, a special equipment is required, either a continuous laser with far red emission (785 nm) promoting photosystem-I-specific fluorescence [20] or immunostaining methods [13].

Another promising method for photosystem co-localization is represented by cryogenic microscopes [25]. With this method, PSI can be detected by its red shifted fluorescence emission from its lowest-energy traps. Basically, there are two types of cryogenic microscopes, in the first the objective lens is immersed in a cooling medium (see e.g. [26,27]), in the second type they are fitted outside the cryostat [28]. In this case, an objective lens with a long working distance is required; they are characterized by lower NA, which limits special resolution and decreases the intensity of the fluorescence signal. Recently [22], some of these disadvantages have been partially overcome by a novel cryogenic microscopic method in which the objective lens was situated inside the adiabatic vacuum space of the cryostat. The approach drastically shortened the working distance, allowing to use semi-conventional objectives with higher NA [22]. However, in this case an adiabatic vacuum sample holder for cryogenic microscope is needed [22]. Here we newly describe a simpler method for PSI and PSII localization that is applicable for commercial confocal microscopes (tested on Olympus FV1000) in combination with a conventional thermal controlled stage Linkam THMSG-600. The experimental approach allowed us to detect the co-localization of phycobilisomes with photosystem I and II simultaneously in single cells of *Anabaena sp. PCC 7120*.

2. Materials and Methods

2.1. Cell Cultures

Anabaena sp. PCC 7120 cells were cultivated in BG 11 medium with optimal nitrogen content (at 18 °C) on a continual light (fluorescent tubes, 40 $\mu\text{mol m}^{-2} \text{s}^{-1}$). For the microscopic imaging the living cells were centrifuged 3 times at 8000 rpm, the pellet was re-suspended in the growing medium.

2.2. The Low Temperature Fluorescence Spectra

The low temperature fluorescence spectra were checked by an Ocean Optics QE Pro spectrometer. Cooling was provided by a Linkam THMSG-600 thermal controlled stage (Linkam Scientific Instruments, Guildford, UK) attached to an upright Olympus BX41 epifluorescence microscope. Excitation was provided by a mercury lamp in a spectral range between 470 nm and 490 nm. (BP470–490 excitation filter and DM505 dichroic mirror was applied – Olympus U-MNIBA2 filter cube for fluorescence microscopy – without the emission of the original filter).

2.3. Confocal Fluorescence Microscopy and Image Processing

The Olympus FV1000 inverted confocal microscope equipped with a long working distance air objective (Olympus MPlan 100x/0.90) was used for confocal imaging in combination with the Linkam THMSG-600 thermal controlled stage (Linkam Scientific Instruments, Guildford, UK) that was modified for our inverted microscope setup. The stage contains a liquid nitrogen cooling system and an internal electrical heater. The cooling rate was 130 K/min, the constant temperature for the measurements was 83 K (closest available temperature to 77 K). The excitation of chlorophyll and phycobilisome fluorescence was carried out with an Ar laser (488 nm) and with a diode laser (635 nm) respectively.

A dichroic mirror DM405/488/559/635 was used and fluorescence emission was detected at 710–750 nm for photosystem I, 690–705 nm for photosystem II and at 650–680 nm for PBS emission. The different spectral ranges were measured during successive scans for every setup separately. The setups were changed by the Cell Finder program we have developed. The program was written in C language and externally controlled the Olympus FV1000 microscope, it was able to change the excitation (lasers) and emission (the spectral ranges of detectors) parameters. The Cell Finder provided special timing functions and control over the whole imaging process allowing us to perform successive scans with different excitations and emissions within a few seconds. The sequence of PSII, PSI, PBS acquisitions was repeated 3 times per position. The stability (immobility) of the sample during scanning was double-checked by the analysis of the images taken from the repeated acquisitions performed at the same positions.

Image processing was performed using the ImageJ 1.47v program [29] and macros we developed for automatic translational corrections and construction of composite images. The FFT (fast Fourier transform) based image cross-correlation method corrected small movements of the cells between the acquired images (maximum 1–2 pixel found). The average images were then constructed from the repeated acquisitions. Then the final RGB composite image was constructed, where red color represented photosystem II emission, green photosystem I emission and blue Phycobilisome emission.

3. Results and Discussion

Initially, we have adapted a commercial temperature stage for the Olympus FV 1000 confocal microscope (see scheme on Fig. 1.) for cryo measurements on an inverted confocal microscope. The motorized microscope stage (Fig. 1, see part “microscopy stage”) was connected to the Linkam sample holder by wooden thermal isolator blocks (Fig. 1, part “ib”), they protected the microscope against cold and held the Linkam sample holder in horizontal position. The sample in agar was situated on the temperature controlled silver blocks (Fig. 1, part “silver block”) inside the Linkam stage (see gray rectangle in Fig. 1). The Z range of the objective was modified properly by an extension tube based on the geometry of the upside down position of Linkam stage.

The water condensation was eliminated by gaseous nitrogen that flew around the sample and the objective (see Fig. 1, gray area). The method was visually tested in order to achieve the minimal efficient N₂ current. The low temperature gaseous N₂ (see gray solid arrow, Fig. 1) was taken from the Linkam pump outlet (Fig. 1 – “pump”) and went through the hollow objective coat to minimize the thermal gradient around the objective.

The optimal final setup we came up with was the following: before every cooling procedure with a new sample, the sample holder was flushed with an intensive flow of gaseous N₂ from the gas bomb. Then, liquid nitrogen from a tank was used for cooling the sample holder silver block (Fig. 1, “silver block”) and a constant mild liquid nitrogen current was provided all over the sample holder (Fig. 1, gray area). The liquid nitrogen exhausted from the pump (Fig. 1, gray solid arrow) then continuously became gaseous and was re-used as a source of cold N₂ inside the objective coat (Fig. 1, “oc”). The output of the nitrogen was provided through a porous plastic isolation ring (Fig. 1, “ir”) situated between the objective (Fig. 1, “obj”) and the protective objective coat (Fig. 1, “oc”). The setup kept the sample and the objective clean, as well as provided a clear field of view for further scanning. Moreover, the setup formed an optimal temperature gradient that kept the sample at low temperature (close to 77 K) and protected the objective.

The temperature of the Linkam sample holder was continuously measured by a thermometer incorporated in the Linkam system. Our system was able to keep a constant temperature around 83 K at the silver block that was supposedly sufficient to see the emission of photosystem I (PSI). The presence of the PSI fluorescence at this temperature was tested with *Anabaena sp. PCC 7120* cells by the upright

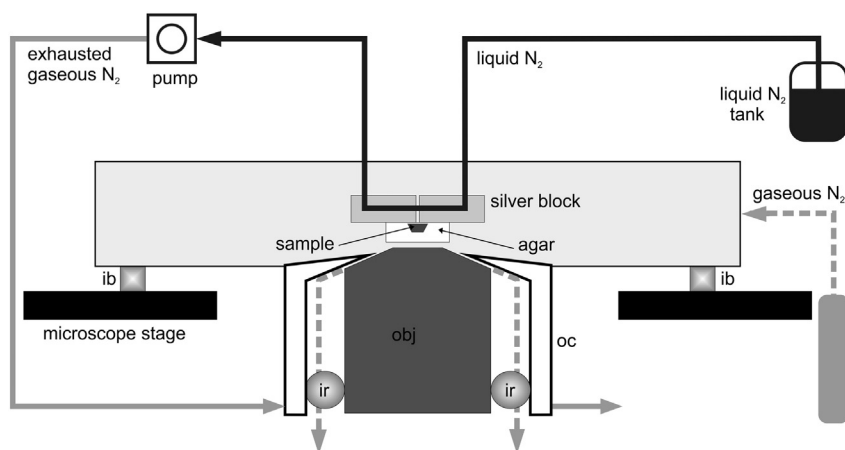


Fig. 1. Modified sample holder arrangement for inverted microscope FV1000. The sample was situated on the temperature controlled cylindrical silver block of the Linkam system and covered by agar gel. The temperature regulation in the silver block was done by the liquid N₂ flow (black) in combination with internal electric heating. The area around the sample was protected against condensation by gaseous N₂ (gray, dashed) inflow. The objective coat (oc) was constantly pumped by exhausted gaseous N₂ (gray) outflowing from the Linkam pump. The sample holder was thermally isolated from the microscope stage by isolator blocks (ib) and from the objective (obj) by a porous plastic isolation ring (ir) that provided output of N₂ from the sample holder.

206 fluorescence microscope in the epifluorescence setup (see Materials
207 and Methods). During the spectra measurement the fluorescence emission
208 that was collected from more cells that brings a different approach
209 in comparison to typical single cell setup (see e.g. [30]). The tempera-
210 Q5 ture of the sample changed from 295 K towards minimal temperature
211 accessible by our system – 79 K. At higher temperatures, there was
212 dominant fluorescence coming from PSII (below 700 nm), the PSI emis-
213 sion above 700 nm became dominant at lower temperatures (Fig. 2).
214 This shows that the low temperature we used in our system (79 K,
215 83 K) enabled the detection of the red-shifted fluorescence of photosys-
216 tem I with typical emission at maximum of 726 nm and at 697 nm for
217 PSII (see Fig. 2). The thermal controlled stage was thus appropriate for
218 confocal microscopy imaging of PSI (between 710–750 nm) and PSII
219 (between 690–705 nm) with excitation 488 nm; the PBS emission
220 was measured consequently in the range 650–680 nm with different
221 excitation (635 nm) in a single-cell setup at 77 K (Fig. 3).

222 Fig. 3 shows cryo-imaging of *Anabaena sp. PCC 7120* cells obtained
223 with the system described above. The figure represents separate pictures
224 from the three independent fluorescence channels reflecting PSII emis-
225 sion (Fig. 3, “PSII” – in red), PSI emission (Fig. 3, “PSI” – in green) and
226 Phycobilisome emission (Fig. 3, “PBS” – in blue). These pictures were

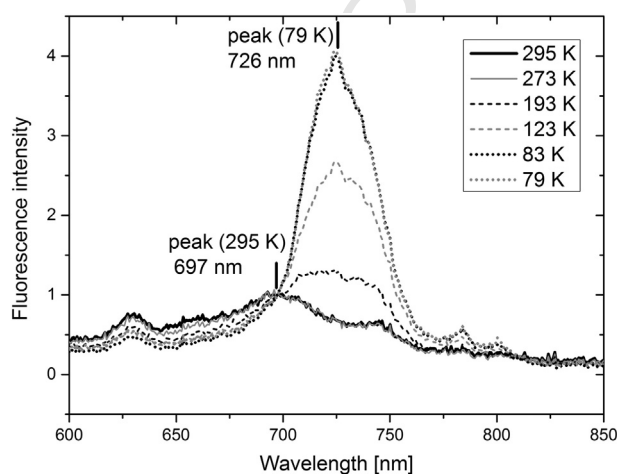


Fig. 2. Fluorescence spectra of *Anabaena sp. PCC 7120* cells measured at different temperatures. Spectra were collected from cells situated on the silver block (see Fig. 1), temperature was controlled by the Linkam system attached to the Olympus BX41 fluorescence microscope. Fluorescence was excited between 470–490 nm by a range filter in the microscope and normalized to 697 nm.

227 then used and the composite image was constructed showing PSI, PSII
228 and PBS colocalization (Fig. 3 – “composite”) from the three independent
229 RGB channels. The composite picture shows the distribution of the photo-
230 synthetic protein complexes. We have found only three dominant types
231 of areas: (1) Area No. 1 – white – with similar pixel intensity from all
232 three channels red–green–blue; (2) Area No. 2 – magenta – where pixel
233 intensity of the red and the blue channels were similar, pixels from the
234 green channel had much lower intensity here; and (3) Area No. 3 –
235 green – where pixels from the green channel were the most intensive.
236 White areas (Area No. 1) thus represent an area containing high level of
237 all three protein complexes we studied (PSI-PSII-PBS), magenta
238 represents areas where PSII were co-localized with PBS antennas (Area
239 No. 2), and the green parts (Area No. 3) of the composite image show

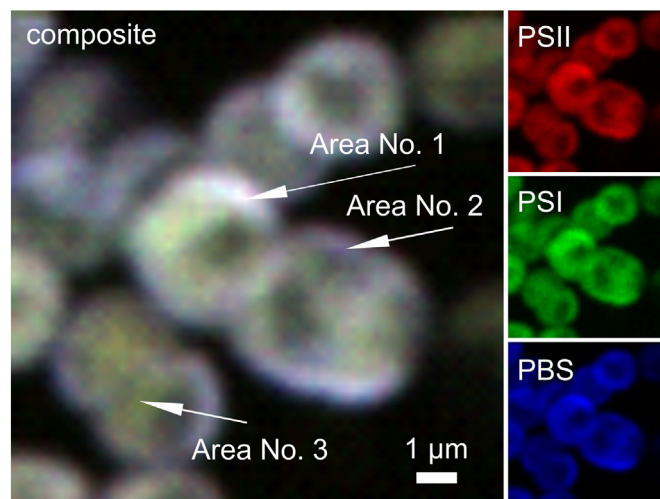


Fig. 3. Typical cryo images of the photosynthetic pigment–protein complexes of *Anabaena sp. PCC 7120* cells. The “composite” image consists of three channels reflecting the fluorescence of PSI, PSII and PBS that were measured simultaneously with the same cells. The single channels were detected with the following setups: PSII fluorescence – red (ex: 488 nm, em: 690–705 nm), PSI fluorescence – green (ex: 488 nm, em: 710–750 nm), PBS fluorescence – blue (ex: 635 nm, em: 650–680 nm). The characteristic areas of different composition are marked by different colors and shown by arrows: Area No. 1 – PSI-PSII-PBS supercomplex (white) with similar pixel intensities from all three channels (red–green–blue); Area No. 2 – PSII-PBS supercomplex (magenta) with similar pixel intensities of the red and blue channels (low intensity of green pixels); Area No. 3 – PSI area (green) where pixels from the green channel were the most intensive. Images were taken at 8 different areas, to increase signal/noise ratio, 9 acquisitions on each area were then taken. Presented data thus represent a typical organization of PSII, PSI, and PBS from pictures we observed.

the part of thylakoids where PSI proteins were in high abundance in comparison to PSII and PBS signals (see Fig. 3 “composite”). The other possible areas including PSI-PBS area (cyan area), PSII only (red area) and free PBS (blue area) were missing from the picture. Even though we were limited by the long working distance objective required for cryogenic measurements (providing 0.32 μm theoretical resolution in x–y due to its relatively low numerical aperture), still, we were able to identify the heterogeneous organization of thylakoid membrane of cyanobacteria. Our data thus shows that the thylakoid membranes of *Anabaena sp. PCC 7120* consist of three dominant areas: an area with the PSI-PSII-PBS supercomplex, an area with dominance of the PSII-PBS supercomplex and an area where mostly PSI was present. We have found some differences in PSI/PSII localization in comparison to previous data obtained with *Synechocystis PCC 6803* [6]. The hyperspectral confocal fluorescence imaging method used in this article has suggested heterogeneity between thylakoid rings; the inner thylakoids were rich in photosystem I. However, our data cannot exclude/confirm this observation due to the limited resolution of our system that is about the size of thylakoid membrane width (ca 300 nm). The interpretation of the heterogeneous organization of PSI and PSII proposed based on hyperspectral confocal fluorescence imaging [24] is limited by a considerable overlap of PBS fluorescence emission with both PSII and PSI fluorescence. In fact, isolated PBS has intense fluorescence emission above 700 nm (see e.g. [31]) that can overlap with PSI emission, that is less dominant at room temperatures [32]. Therefore, our cryo-imaging of PSI and PSII, with the new setup, can overcome the limitation by measurements at low temperature, when PBS emission above 700 nm is much lower [31] and red-shifted PSI emission is dominant [32]. Our data clearly show separated areas preferentially containing PSI (see green “Area No. 3” in Fig. 3.) and PSII with PBS (see magenta “Area No. 2” in Fig. 3.) and a third area containing all pigmented protein complexes PBS-PSI-PSII (see green “Area No. 3” in Fig. 3.) in filamentous *Anabaena sp. PCC 7120* cells.

The heterogeneous organization of photosystems we observed in *Anabaena sp. PCC 7120* (Fig. 3) and that has been already shown in *Synechocystis sp. PCC 6803* [4–6] resembles heterogeneity typical for higher plants' thylakoids, with stromal and granal thylakoids abundant in PSI and PSII respectively [1]. The heterogeneous organization of proteins in biological membranes seems to be a common feature of biological membranes including thylakoid membrane. The original fluid-mosaic-model proposed a rather homogenous organization [33] that is currently redrawn and membranes are considered as heterogeneous structures containing specialized areas, some of them with rather restricted mobility (see recent review [34]). Indeed, unequal protein distribution in cells has been already detected also for cyanobacteria proteins including circadian clock proteins [35], proteases [36,37] or for respiratory complexes [38]. Segregated bioenergetics domains for photosynthetic proteins have also been shown in cyanobacteria *Gloeobacter violaceus* [39] representing the primitive rock dwelling organism [40] without thylakoids. However, thylakoid localization of some processes into specialized domains has been already proposed, it includes restriction of plastoquinone diffusion between PSII and cytochrome b6f into domains [41,42] or the presence of protein biogenesis in specialized areas [43].

The heterogeneous organization of pigmented proteins in thylakoids of cyanobacteria *Anabaena sp. PCC 7120* we observed (Fig. 3) probably also affects physiological processes in cyanobacteria cells like protein mobility (for recent review see [44]) or state transitions, a process equilibrating excitation delivery from PBS to photosystems (for recent review see e.g. [45]). In fact, our data have identified only two types of PBS interaction with photosystems: (1) thylakoid membrane area with PBS together with both photosystems, PSI and PSII (see Area No. 1 in Fig. 3) reflecting probably the recently isolated PSI-PSII-PBS supercomplex [17]; and (2) membrane area with PBS and PSII only (see Area No. 2 in Fig. 3). However, there was almost no cyan color in the composite image (Fig. 3). We can thus hypothesize that state transitions probably do not involve long-distance PBS redistribution between

the “PSI areas” (Area No. 3) and the “PSII areas” (Area No. 2) as a supercomplex of PBS and PSI is not present in native *Anabaena sp. PCC 7120*. These data speak in favor of a mechanism of state transition that requires only a slight rearrangement in the PBS-PSI-PSII supercomplex without long-distance phycobilisome mobility (for recent review see [45]). It also does not exclude involvement of other mechanisms like phycobilisomes decoupling [46,47]. However, to confirm all those hypotheses directly, more experimental data are required.

4. Conclusions

We have shown that the commercial thermal controlled sample holder can be adapted for inverted confocal microscopes in order to investigate photosynthetic proteins in vivo. The cryo-imaging of *Anabaena sp. PCC 7120* cells has indicated a heterogeneous organization in native thylakoid membranes with dominant areas represented by PSI-PSII-PBS supercomplex, by PSI area and by PSII-PBS area. Our data showed the applicability of this simple experimental approach to access thylakoid membrane organization in a small cyanobacteria cell and thus it is promising for the co-localization of the photosystems in any single cell photosynthetic organism.

Acknowledgments

Our research was supported by the Czech Science Foundation (project GAČR P501–12–0304), by institutional projects provided by the Czech Ministry of Education, Youth and Sport, project Algain (EE2.3.30.0059) and by institutional projects Algatech (CZ.1.05/2.1.00/03.0110) and Algatech Plus (MSMT LO1416). We would like to thank Ondřej Komárek for his technical assistance during cell cultivation.

References

1. L. Mustardy, K. Buttle, G. Steinbach, G. Garab, The three-dimensional network of the thylakoid membranes in plants: quasi-helical model of the granum–stroma assembly, *Plant Cell* 20 (2008) 2552–2557.
2. M. Yokono, A. Takabayashi, S. Akimoto, A. Tanaka, A megacomplex composed of both photosystem reaction centres in higher plants, *Nat. Commun.* 6 (2015).
3. B.D. Engel, M. Schaffer, K.L. Cuellar, E. Villa, J.M. Plitzko, W. Baumeister, Native architecture of the *Chlamydomonas* chloroplast revealed by in situ cryo-electron tomography, *eLife* (2015).
4. A.M. Collins, M. Liberton, H.D.T. Jones, O.F. Garcia, H.B. Pakrasi, J.A. Timlin, Photosynthetic pigment localization and thylakoid membrane morphology are altered in *Synechocystis* 6803 phycobilisome mutants, *Plant Physiol.* 158 (2012) 1600–1609.
5. M. Liberton, A.M. Collins, L.E. Page, W.B. O'Dell, H. O'Neill, V.S. Urban, J.A. Timlin, H.B. Pakrasi, Probing the consequences of antenna modification in cyanobacteria, *Photosynth. Res.* 118 (2013) 17–24.
6. W.F.J. Vermaas, J.A. Timlin, H.D.T. Jones, M.B. Sinclair, L.T. Nieman, S.W. Hamad, D.K. Melgaard, D.M. Haaland, In vivo hyperspectral confocal fluorescence imaging to determine pigment localization and distribution in cyanobacterial cells, *Proc. Natl. Acad. Sci. U. S. A.* 105 (2008) 4050–4055.
7. M. Iwai, M. Yokono, A. Nakano, Visualizing structural dynamics of thylakoid membranes, *Sci. Rep.* 4 (2014).
8. H. Kirchhoff, C. Hall, M. Wood, M. Herbstova, O. Tsabari, R. Nevo, D. Charuvi, E. Shimoni, Z. Reich, Dynamic control of protein diffusion within the granal thylakoid lumen, *Proc. Natl. Acad. Sci. U. S. A.* 108 (2011) 20248–20253.
9. B. Daum, D. Nicastro, J.A. II, J.R. McIntosh, W. Kuhlbrandt, Arrangement of photosystem II and ATP synthase in chloroplast membranes of spinach and pea, *Plant Cell* 22 (2010) 1299–1312.
10. C.W. Mullineaux, Function and evolution of grana, *Trends Plant Sci.* 10 (2005) 521–525.
11. H.W. Trissl, C. Wilhelm, Why do thylakoid membranes from higher-plants form grana stacks, *Trends Biochem. Sci.* 18 (1993) 415–419.
12. I.M. Folea, P. Zhang, E.M. Aro, E.J. Boekema, Domain organization of photosystem II in membranes of the cyanobacterium *Synechocystis PCC6803* investigated by electron microscopy, *FEBS Lett.* 582 (2008) 1749–1754.
13. D.M. Sherman, T.A. Troyan, L.A. Sherman, Localization of membrane-proteins in the cyanobacterium *Synechococcus sp. Pcc7942* – radial asymmetry in the photosynthetic complexes, *Plant Physiol.* 106 (1994) 251–262.
14. M. Schottkowski, M. Peters, Y. Zhan, O. Rifai, Y. Zhang, W. Zerges, Biogenic membranes of the chloroplast in *Chlamydomonas reinhardtii*, *Proc. Natl. Acad. Sci.* 109 (2012) 19286–19291.
15. O. Vallon, F.A. Wollman, J. Olive, Distribution of intrinsic and extrinsic subunits of the PS II protein complex between appressed and non-appressed regions of the thylakoid membrane: an immunocytochemical study, *FEBS Lett.* 183 (1985) 245–250.

- 374 [16] R. Nevo, D. Charuvi, E. Shimoni, R. Schwarz, A. Kaplan, I. Ohad, Z. Reich, Thylakoid mem-
375 brane perforations and connectivity enable intracellular traffic in cyanobacteria, *EMBO*
376 *J.* 26 (2007) 1467–1473.
- 377 [17] H. Liu, H. Zhang, D.M. Niedzwiedzki, M. Prado, G. He, M.L. Gross, R.E. Blankenship,
378 Phycobilisomes supply excitations to both photosystems in a megacomplex in
379 cyanobacteria, *Science* 342 (2013) 1104–1107.
- 380 [18] R. Yokoo, R. Hood, D. Savage, Live-cell imaging of cyanobacteria, *Photosynth. Res.*
381 126 (2015) 33–46.
- 382 [19] S. Caffarri, T. Tibiletti, R.C. Jennings, S. Santabarbara, A comparison between plant
383 photosystem I and photosystem II architecture and functioning, *Curr. Protein Pept.*
384 *Sci.* 15 (2014) 296–331.
- 385 [20] M. Hasegawa, T. Yoshida, M. Yabuta, M. Terazima, S. Kumazaki, Anti-stokes fluores-
386 cence spectra of chloroplasts in *Parachlorella kessleri* and maize at room temperature
387 as characterized by near-infrared continuous-wave laser fluorescence microscopy
388 and absorption microscopy, *J. Phys. Chem. B* 115 (2011) 4184–4194.
- 389 [21] S. Kumazaki, M. Akari, M. Hasegawa, Transformation of thylakoid membranes dur-
390 ing differentiation from vegetative cell into heterocyst visualized by microscopic
391 spectral imaging, *Plant Physiol.* 161 (2013) 1321–1333.
- 392 [22] Y. Shibata, W. Katoh, T. Chiba, K. Namie, N. Ohnishi, J. Minagawa, H. Nakanishi, T.
393 Noguchi, H. Fukumura, Development of a novel cryogenic microscope with numer-
394 ical aperture of 0.9 and its application to photosynthesis research, *Biochim. Biophys.*
395 *Acta Bioenerg.* 1837 (2014) 880–887.
- 396 [23] M. Hasegawa, T. Shiina, M. Terazima, S. Kumazaki, Selective excitation of photosys-
397 tems in chloroplasts inside plant leaves observed by near-infrared laser-based fluo-
398 rescence spectral microscopy, *Plant Cell Physiol.* 51 (2010) 225–238.
- 399 [24] M.B. Sinclair, D.M. Haaland, J.A. Timlin, H.D. Jones, Hyperspectral confocal micro-
400 scope, *Appl. Opt.* 45 (2006) 6283–6291.
- 401 [25] K. Sugiura, S. Itoh, Single-cell confocal spectrometry of a filamentous *Cyanobacterium*
402 *nostoc* at room and cryogenic temperature. Diversity and differentiation of pigment
403 systems in 311 cells, *Plant Cell Physiol.* 53 (2012) 1492–1506.
- 404 [26] A.M. van Oijen, M. Ketelaars, J. Kohler, T.J. Aartsma, J. Schmidt, Spectroscopy of single
405 light-harvesting complexes from purple photosynthetic bacteria at 1.2 K, *J. Phys.*
406 *Chem. B* 102 (1998) 9363–9366.
- 407 [27] P. Tamarat, A. Maali, B. Lounis, M. Orrit, Ten years of single-molecule spectroscopy, *J.*
408 *Phys. Chem. A* 104 (2000) 1–16.
- 409 [28] F. Vacha, V. Sarafis, Z. Benediktyova, L. Bumba, J. Valenta, M. Vacha, C.R. Sheue, L.
410 Nedbal, Identification of photosystem I and photosystem II enriched regions of thy-
411 lakoid membrane by optical microimaging of cryo-fluorescence emission spectra
412 and of variable fluorescence, *Micron* 38 (2007) 170–175.
- 413 [29] C.A. Schneider, W.S. Rasband, K.W. Eliceiri, NIH Image to ImageJ: 25 years of image
414 analysis, *Nat. Methods* 9 (2012) 671–675.
- 415 [30] L. Ying, X. Huang, B. Huang, J. Xie, J. Zhao, X. Sheng Zhao, Fluorescence emission and
416 absorption spectra of single *Anabaena sp.* strain PCC7120 cells, *Photochem.*
417 *Photobiol.* 76 (2002) 310–313.
- 418 [31] D. Jallet, M. Gwizdala, D. Kirilovsky, ApcD, ApcF and ApcE are not required for the
419 orange carotenoid protein related phycobilisome fluorescence quenching in the cy-
420 anobacterium *Synechocystis* PCC 6803, *Biochim. Biophys. Acta Bioenerg.* 1817
421 (2012) 1418–1427.
- 422 [32] E.G. Andrizhiyevskaya, A. Chojnicka, J.A. Bautista, B.A. Diner, R. van Grondelle, J.P.
423 Dekker, Origin of the F685 and F695 fluorescence in photosystem II, *Photosynth.*
424 *Res.* 84 (2005) 173–180.
- 425 [33] S.J. Singer, G.L. Nicolson, Fluid mosaic model of structure of cell-membranes, *Science*
426 175 (1972) 720–8.
- 427 [34] G.L. Nicolson, The fluid–mosaic model of membrane structure: still relevant to un-
428 derstanding the structure, function and dynamics of biological membranes after
429 more than 40 years, *Biochim. Biophys. Acta Biomembr.* 1838 (2014) 1451–1466.
- 430 [35] Susan E. Cohen, Marcella L. Erb, J. Selimkhanov, G. Dong, J. Hasty, J. Pogliano, Susan S.
431 Golden, Dynamic localization of the cyanobacterial circadian clock proteins, *Curr.*
432 *Biol.* 24 (2014) 1836–1844.
- 433 [36] V. Krynicka, M. Tichy, J. Krafl, J.F. Yu, R. Kana, M. Boehm, P.J. Nixon, J. Komenda, Two
434 essential FtsH proteases control the level of the Fur repressor during iron deficiency
435 in the cyanobacterium *Synechocystis sp* PCC 6803, *Mol. Microbiol.* 94 (2014) 435
436 609–624.
- 437 [37] J. Sacharz, S.J. Bryan, J. Yu, N.J. Burroughs, E.M. Spence, P.J. Nixon, C.W. Mullineaux,
438 Sub-cellular location of FtsH proteases in the cyanobacterium *Synechocystis sp.*
439 PCC 6803 suggests localised PSII repair zones in the thylakoid membranes, *Mol.*
440 *Microbiol.* 96 (2015) 448–462.
- 441 [38] L.-N. Liu, S.J. Bryan, F. Huang, J. Yu, P.J. Nixon, P.R. Rich, C.W. Mullineaux, Control of
442 electron transport routes through redox-regulated redistribution of respiratory
443 complexes, *Proc. Natl. Acad. Sci. U. S. A.* 109 (2012) 11431–11436.
- 444 [39] S. Rexroth, C.W. Mullineaux, D. Ellinger, E. Sendtko, M. Rogner, F. Koenig, The plasm-
445 ma membrane of the cyanobacterium *Gloeobacter violaceus* contains segregated bio-
446 energetic domains, *Plant Cell* 23 (2011) 2379–2390.
- 447 [40] J. Mareš, P. Hrouzek, R. Kaňa, S. Ventura, O. Strunecký, J. Komárek, The primitive
448 thylakoid-less cyanobacterium *Gloeobacter* is a common rock-dwelling organism, *PLoS*
449 *One* 8 (2013), e66323.
- 450 [41] H. Kirchhoff, S. Horstmann, E. Weis, Control of the photosynthetic electron transport
451 by PQ diffusion microdomains in thylakoids of higher plants, *Biochim. Biophys. Acta*
452 *Bioenerg.* 1459 (2000) 148–168.
- 453 [42] J. Lavergne, J.P. Bouchaud, P. Joliot, Plastoquinone compartmentation in chloro-
454 plants.2. Theoretical aspects, *Biochim. Biophys. Acta* 1101 (1992) 13–22.
- 455 [43] J. Nickelsen, W. Zerges, Thylakoid biogenesis has joined the new era of bacterial cell
456 biology, *Front. Plant Sci.* 4 (2013) 458.
- 457 [44] R. Kaňa, Mobility of photosynthetic proteins, *Photosynth. Res.* 116 (2013) 465–479.
- 458 [45] D. Kirilovsky, R. Kaňa, O. Prášil, Mechanisms modulating energy arriving at reaction
459 centers in cyanobacteria, in: B. Demmig-Adams, G. Garab, W. Adams Iii, Govindjee
460 (Eds.), *Non-Photochemical Quenching and Energy Dissipation in Plants, Algae and*
461 *Cyanobacteria*, Springer, Netherlands 2014, pp. 471–501.
- 462 [46] V. Chukhutsina, L. Bersanini, E.-M. Aro, H. van Amerongen, Cyanobacterial light-
463 harvesting phycobilisomes uncouple from photosystem I during dark-to-light tran-
464 sitions, *Sci. Rep.* 5 (2015) 14193.
- 465 [47] R. Kaňa, O. Prášil, O. Komárek, G.C. Papageorgiou, Govindjee, Spectral characteristic
466 of fluorescence induction in a model cyanobacterium, *Synechococcus sp* (PCC 7942),
467 *Biochim. Biophys. Acta* 1787 (2009) 1170–1178.